Synthesis, Characterization, and Reactivity of Chromium Boratabenzene Complexes

Jonathan S. Rogers, Xianhui Bu, and Guillermo C. Bazan*

Department of Chemistry, University of California, Santa Barbara, California 93106

Received May 1, 2000

In contrast to the reactivity observed with the isoelectronic cyclopentadienyl salts, the reaction of $CrCl_3(THF)_3$ with boratabenzene anions results in the formation of Cr(II) complexes. Thus, addition of Li(C_5H_5B-Me) to $CrCl_3(THF)_3$ in THF gives $(C_5H_5B-Me)_2Cr$ (**3**). Similarly, Li($C_5H_5B-NMe_2$) and $CrCl_3(THF)_3$ yield $(C_5H_5B-NMe_2)_2Cr$ (**4**), while Li(C_5H_5B-Ph) and $CrCl_3(THF)_3$ provide $(C_5H_5B-Ph)_2Cr$ (**5**). Compounds **3**−**5** were characterized by single-crystal X-ray diffraction studies, and all possess typical sandwich structures. The reaction of borabenzene−ligand adducts with suitable Cr(III) starting materials provides boratabenzene−Cr(III) complexes. Addition of $C_5H_5B-PMe_3$ (**Bb**-PMe_3) to $MeCrCl_2(THF)_3$ in benzene gives $(C_5H_5B-Me)CrCl_2(PMe_3)$ (**6**) in low yield. Treatment of $MeCrCl_2(THF)_3$ with the pyridine adduct of borabenzene, $C_5H_5B-NC_5H_5$ (**Bb**-Py), does not work effectively. The composition of one of the products from this reaction, the binuclear dimer $[(C_5H_5B-Me)CrClMe]_2$ (**7**), indicates Me/Cl redistribution processes. Treatment of $CrCl_3(THF)_3$ with 3 equivalents MeMgBr in THF, followed by addition of **Bb**-Py gives $(C_5H_5B-Me)CrMe_2(Py)$ (**8**). Similarly, $Ph_3Cr(THF)_3$ and **Bb**-Py afford $(C_5H_5B-Ph)CrPh_2(Py)$ (**9**). Compound **8** with the well-defined activators $B(C_6F_5)_3$ and $[Ph_3C][B(C_6F_5)_4]$ can polymerize ethylene with activities competitive with those of $(C_5H_5B-Me)CrMe_2(PMe_3)/B(C_6F_5)_3$ (**2**/$B(C_6F_5)_3$) and $Cp^*CrMe_2(PMe_3)/B(C_6F_5)_3$. Methylaluminoxane (MAO) can also be used as an activator with the complexes containing a coordinated phosphine. The pyridine counterparts fail to give polymerization catalysts with MAO.

Introduction

Olefin polymerization catalysts based on chromium are used in large-scale industrial processes.[1] The Phillips catalyst is a heterogeneous mixture prepared by impregnation of silica with chromium oxides and is widely used to prepare linear polyethylene.[2] Catalysts formed by adsorption of chromocene on silica have also been used by Union Carbide.[3] The ill-defined nature of these mixtures has prompted considerable efforts to develop well-defined homogeneous catalysts in the hope of rationally controlling the reactivity at chromium by ligand design. Theopold's pioneering work on complexes exemplified by $[Cp^*CrMe(THF)_2][BPh_4]$ ($Cp^* = C_5Me_5$), which are ethylene polymerization catalysts, is particularly noteworthy.[4] Research teams in industry and academia continue to expand the structural diversity and utility of chromium-based polymerization catalysts.[5]

In connection to our work with boratabenzene complexes of zirconium, we recently reported on boratabenzene complexes of Cr(III).[6] We were motivated by the fact that the reactivities of boratabenzene zirconium catalysts are modulated by the electronic properties of the boron substituent.[7] Thus far, the synthesis of the boratabenzene−Cr(III) species requires the reaction of borabenzene adducts[8] with alkyl and phenyl complexes of chromium. For example, $(C_5H_5B-Ph)CrPh_2(PMe_3)$ (**1**) is produced when $C_5H_5B-PMe_3$ (**Bb**−PMe_3) and $Ph_3Cr(THF)_3$[9] react with each other in toluene, as shown in eq 1.

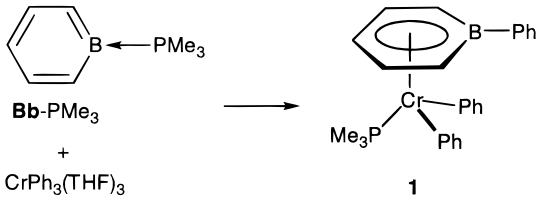

(1)

Similarly, "$CrMe_3$", produced in situ by treating $CrCl_3(THF)_3$ with 3 equiv of MeMgBr, reacts with **Bb**−PMe_3 to give $(C_5H_5B-Me)CrMe_2(PMe_3)$ (**2**), as shown in eq 2.

(1) Parshall, G. W.; Ittel, S. D., *Homogeneous Catalysis*, 2nd ed.; Wiley: New York, 1992.
(2) Clark, A.; Hogan, J. P., Banks, R. L.; Lanning, W. C. *Ind. Eng. Chem.* **1956**, *48*, 1152.
(3) Karol, F. J.; Karapinka, G. L.; Wu, C.; Dow, A. W.; Johnson, R. N.; Carrick, W. L. *J. Polym. Sci. A* **1972**, *10*, 2621.
(4) (a) Theopold, K. H. *CHEMTECH* **1997**, 26, and references therein. (b) Thomas, B. J.; Noh, S. N.; Schulte, G. K.; Sendlinger, S. C.; Theopold, K. H. *J. Am. Chem. Soc.* **1991**, *113*, 893.
(5) (a) Kim, W.; Fevola, M. J.; Liable-Sands, L. M.; Rheingold, A. L.; Theopold, K. H. *Organometallics* **1998**, *17*, 4541. (b) Dohring, A.; Gohre, J.; Jolly, P. W.; Kryger, B.; Rust, J.; Verhovnik, G. P. J. *Organometallics* **2000**, *19*, 388.
(6) Rogers, J. S.; Bu, X.; Bazan, G. C. *J. Am. Chem. Soc.* **2000**, *122*, 730.
(7) (a) Bazan, G. C.; Rodriguez, G.; Ashe, A. J., III.; Al-Ahmad, S.; Müller, C. *J. Am. Chem. Soc.* **1996**, *118*, 2291. (b) Bazan, G. C.; Rodriguez, G.; Ashe, A. J., III.; Al-Ahmad, S.; Kampf, J. W. *Organometallics* **1997**, *16*, 2492. (c) Rogers, J. S.; Bazan, G. C.; Sperry, C. K. *J. Am. Chem. Soc.* **1997**, *119*, 9305. (d) Barnhart, R. W.; Bazan, G. C.; Mourey, T. *J. Am. Chem. Soc.* **1998**, *120*, 1082. (e) Rogers, J. S.; Lachicotte, R. J.; Bazan, G. C. *J. Am. Chem. Soc.* **1999**, *121*, 1288.
(8) (a) Boese, R.; Finke, N.; Henkelmann, J.; Maier, G.; Paetzold, P.; Reisenauer, H. P.; Schmid, G. *Chem. Ber.* **1985**, *118*, 1644. (b) Hoic, D. A.; Wolf, J. R.; Davis, W. M.; Fu, G. C. *Organometallics* **1996**, *15*, 1315.
(9) Herwig, W.; Zeiss, H. H. *J. Am. Chem. Soc.* **1957**, *79*, 6561.

10.1021/om0003685 CCC: $19.00
Publication on Web 08/19/2000

In the presence of typical metallocene activators,[10] complexes **1** and **2** can be converted into ethylene polymerization catalysts.

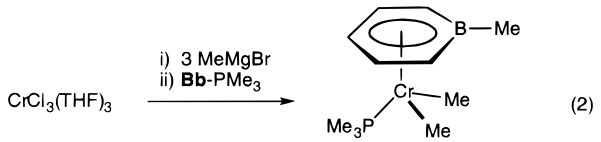

2

In this contribution we provide complete details of our studies concerned with the synthesis and reactivity of Cr(III) boratabenzene complexes. We show that various boratabenzene salts result in reduction of chromium. Next, we examine the preparation of new complexes based on reactivity analogous to that in eqs 1 and 2. Finally, the ethylene polymerization aptitude of Cr(III) boratabenzene catalysts is presented.

Results and Discussion

Reactions with Boratabenzene Anions. Despite their isoelectronic relationship,[11] the chemistries of boratabenzene and cyclopentadienide (Cp) differ greatly upon reaction with readily available chromium(III) starting materials. Slow addition of LiCp (Cp = C_5H_5) to $CrCl_3(THF)_3$ in THF at room temperature (eq 3) is known to provide Cr(III) cyclopentadienyl complexes in good yield.[12]

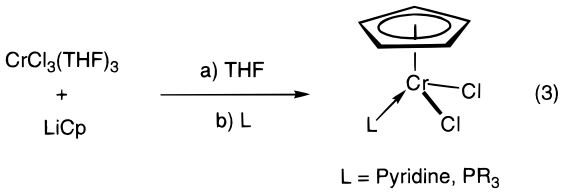

A similar approach using a 1:1 ratio of Li(C_5H_5B−Me) and $CrCl_3(THF)_3$ in THF results in the immediate formation of a brown solution. Removal of solvent, extraction with pentane, and recrystallization leads to (C_5H_5B−Me)$_2$Cr (**3**). Compound **3** was previously pre-

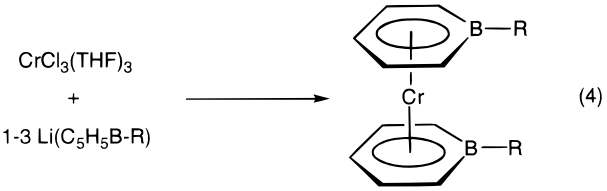

3, R = Me
4, R = NMe_2
5, R = Ph

pared by Herberich, using multiple equivalents of the anion to reduce $CrCl_3$.[13] Crystals of **3** suitable for X-ray diffraction work were grown by slowly cooling a pentane solution to −35 °C, and the results of this study are shown in Figure 1. The complex adopts the parallel sandwich structure typical of chromocenes[14] and exists in an anti configuration in the solid state with a crystallographically imposed C_2 axis. The bonding of the (C_5H_5B−Me) ring and the Cr atom in **3** is similar to that

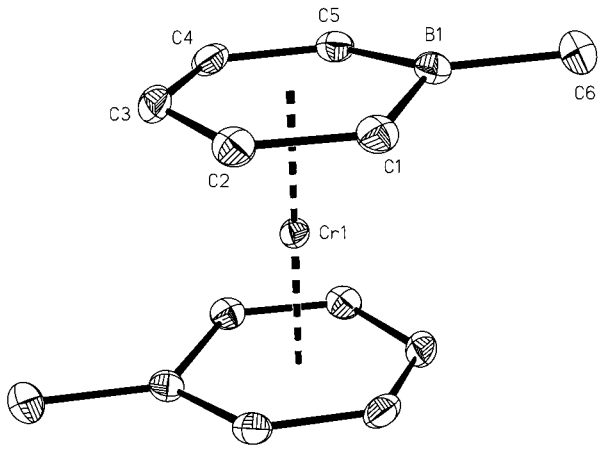

Figure 1. ORTEP view of **3**. Thermal ellipsoids are shown at the 30% probability level; hydrogen atoms were omitted for clarity. Select bond distances (Å): Cr(1)−B(1), 2.365(2); Cr(1)−C(1), 2.197(2); Cr(1)−C(2), 2.174(2); Cr(1)−C(3), 2.185(2); Cr(1)−C(4), 2.172(2); Cr(1)−C(5), 2.196(2); B(1)−C(6), 1.584(3).

in **2**, except that the rings are held in closer proximity to the metal (d(Cr−C_{av}) = 2.185(2) Å in **3** vs d(Cr−C_{av}) = 2.357(2) Å in **2**; d(Cr−B_{av}) = 2.365(2) Å for **3** and d(Cr−B) = 2.481(2) Å for **2**). A contraction in the metal−boron distance with decreasing oxidation state is also observed in the case of (C_5H_5B−N(iPr)$_2$)$_2$ZrCl_2 (d(Zr−B) = 2.980(7) Å) and (C_5H_5B−N(iPr)$_2$)$_2$Zr(PMe_3)$_2$ (d(Zr−B) = 2.830(3) Å).[15]

It is well-documented that boratabenzene ligands are poorer donors for transition metals than their cyclopentadienyl counterparts[16] and, thus, would be expected to favor the lower oxidation states of the metal.[17] Also known is that the electron-donating abilities of boratabenzene ligands can be modified by the choice of boron substitiuent.[18] Dialkylamino groups provide for excellent N−B orbital overlap and allow the metal to bind more strongly to the electron-rich carbon atoms of the ring.[19] Performing the reaction in eq 4 using Li(C_5H_5B−NMe_2), however, also results in reduction of the metal and subsequent formation of (C_5H_5B−NMe_2)$_2$-Cr (**4**). Compound **4** can be isolated in 60% yield after

(10) For reviews of group 4 polymerization catalysts, see: (a) Brintzinger, H. H.; Fischer, D.; Mülhaupt, R.; Rieger, B.; Waymouth, R. M. *Angew. Chem., Int. Ed. Engl.* **1995**, *34*, 1143. (b) *Transition Metals and Organometallics as Catalysts for Olefin Polymerization*; Kaminsky, W., Sinn, H., Eds.; Springer-Verlag: Berlin, 1988. (c) *Ziegler Catalysts*; Fink, G., Mülhaupt, R., Brintzinger, H. H., Eds.; Springer-Verlag: Berlin, 1995. (d) *Metallocenes*; Togni, A., Halterman, R. L., Eds.; Wiley-VCH: New York, 1998. (e) Britovsek, G. J. P.; Gibson, V. C.; Wass, D. F. *Angew. Chem., Int. Ed.* **1999**, 429. (f) Bochmann, M. *J. Chem. Soc., Dalton Trans.* **1996**, *3*, 255.

(11) Ashe, A. J., III.; Al-Ahmad, S.; Fang, X. G. *J. Organomet. Chem.* **1999**, *581*, 92 and references therein.

(12) Richeson, D. S.; Mitchell, J. F.; Theopold, K. H. *Organometallics* **1989**, *8*, 2570.

(13) Herberich, G. E.; Koch, W. *Chem. Ber.* **1977**, *110*, 816.

(14) (a) Flower, K. R.; Hitchcock, P. B. *J. Organomet. Chem.* **1996**, *507*, 275. (b) Blumel, J.; Herker, M.; Hiller, W.; Kohler, F. H. *Organometallics* **1996**, *15*, 3474.

(15) Ashe, A. J., III; Al-Ahmad, S.; Kampf, J. W.; Young, V. G. *Angew. Chem., Int. Ed. Engl.* **1997**, *36*, 2014.

(16) Herberich, G. H.; Ohst, H. *Adv. Organomet. Chem.* **1986**, *25*, 199.

(17) Sperry, C. K.; Bazan, G. C.; Cotter, W. D. *J. Am. Chem. Soc.* **1999**, *121*, 1513.

(18) Bazan, G. C.; Cotter, W. D.; Komon, Z. J. A.; Lee, R. A.; Lachicotte, R. J. *J. Am. Chem. Soc.* **2000**, *122*, 1371.

(19) Bazan, G. C.; Rodriguez, G.; Ashe, A. J., III; Al-Ahmad, S.; Müller, C. *J. Am. Chem. Soc.* **1996**, *118*, 2291.

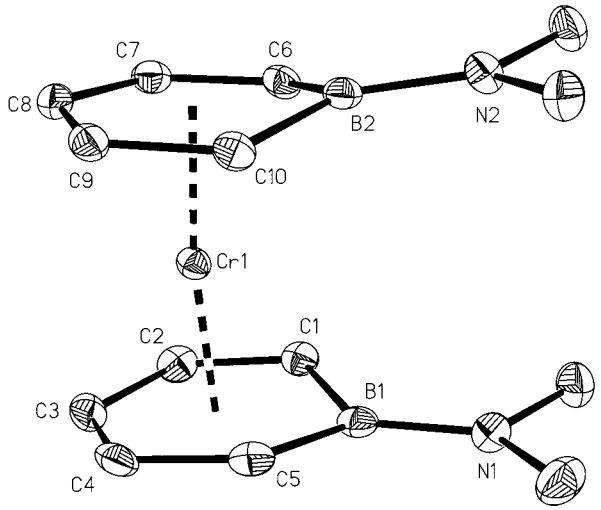

Figure 2. ORTEP view of **4**. Thermal ellipsoids are shown at the 30% probability level; hydrogen atoms were omitted for clarity. Select bond distances (Å): Cr(1)−B(1), 2.419(2); Cr(1)−C(1), 2.200(2); Cr(1)−C(2), 2.183(2); Cr(1)−C(3), 2.190(2); Cr(1)−C(4), 2.177(2); Cr(1)−C(5), 2.196(2); B(1)−N(1), 1.417(3); Cr(1)−B(2), 2.450(2); Cr(1)−C(6), 2.191(2); Cr(1)−C(7), 2.172(2); Cr(1)−C(8), 2.189(2); Cr(1)−C(9), 2.171(2); Cr(1)−C(10), 1.197(2); B(2)−N(2), 1.419(3).

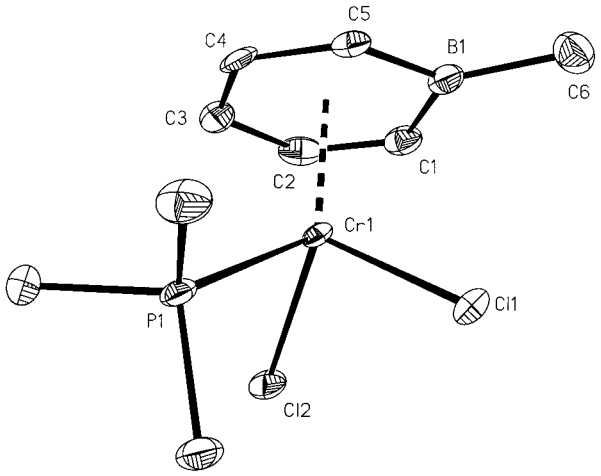

Figure 3. ORTEP view of **6**. Thermal ellipsoids are shown at the 30% probability level; hydrogen atoms were omitted for clarity. Select bond distances (Å): Cr(1)−B(1), 2.494(5); Cr(1)−C(1), 2.339(5); Cr(1)−C(2), 2.299(5); Cr(1)−C(3), 2.258(5); Cr(1)−C(4), 2.301(4); Cr(1)−C(5), 2.332(4); B(1)−C(6), 1.577(7); Cr(1)−Cl(1), 2.2759(13); Cr(1)−Cl(2), 2.2824(13); Cr(1)−P(1), 2.4126(13).

crystallization from pentane as bright red crystals. An X-ray diffraction study of **4** was conducted, and the results are shown in Figure 2. In contrast to **3**, this complex crystallizes with boron substituents in a syn conformation. The bonding observed in **4** is very similar to that of **3**; however, the complex adopts a slightly bent sandwich structure (∠Cent−Cr−Cent = 172.2(1)°). Slightly longer Cr−B distances are also observed in **4** (d(Cr−B_{av}) = 2.435(2) Å), as well as significant boron−nitrogen overlap (d(B−N_{av}) = 1.418(3) Å), typical of other aminoboratabenzene complexes.[20] The reaction involving Li(C_5H_5B−Ph) and $CrCl_3(THF)_3$ also produces the Cr(II) product (C_5H_5B−Ph)$_2$Cr[13] (**5**), and the molecular structure is provided in the Supporting Information.

Several variations of eq 4 were studied with boratabenzene anions but failed to provide the desired Cr(III) species. Conditions examined include lower temperature, the use of nondonor solvents such as toluene and pentane, and pretreatment of $CrCl_3(THF)_3$ with stronger donors such as PMe_3 and pyridine (Py). We sought to reduce the propensity of the boratabenzene anion for electron transfer by exchange with softer cations, which would favor a more covalent interaction. Reagents used for this purpose include $ZnCl_2$, $AlCl_3$, $MgCl_2$, and Me_3SnCl. None of these anion surrogates results in the formation of crystalline product upon reacting with either $CrCl_3(THF)_3$ or $MeCrCl_2(THF)_3$,[21] in donor or nondonor solvents. It may be that some of these reactions produced Cr(III) complexes in low yield. However, without the aid of NMR spectroscopy or the formation of products with considerable solubility differences, it is difficult to gauge the success of these reactions. It is interesting to note that Cr(acac)$_3$ and M(C_5H_5B−R) (acac = 2,4-acetylacetonate; R = NMe_2, OEt; M = Li, Na) do not react in either THF or toluene.

Reactions of Bb−PMe_3 and Bb−Py with $MeCrCl_2(THF)_3$. It seemed logical that the strategy of using borabenzene adducts, as shown in eqs 1 and 2, would be successful using other known complexes of Cr(III) with σ-ligands. The reaction of **Bb**−PMe_3 with $MeCrCl_2(THF)_3$ in benzene occurs immediately and results in a color change from green to dark blue-green. After the reaction is allowed to proceed for 5 min, the solvent was removed to afford a blue-green semisolid. Fractions were then collected by using solvents of different polarity. The pentane fraction contained undesired impurities. Dark blue crystals were obtained by cooling the toluene fraction to −35 °C, and these analyze correctly for $C_9H_{17}BCl_2CrP$. A single-crystal X-ray study (Figure 3) confirms that the product is (C_5H_5B−Me)$CrCl_2(PMe_3)$ (**6**), as shown in eq 5. The overall yield of this reaction is

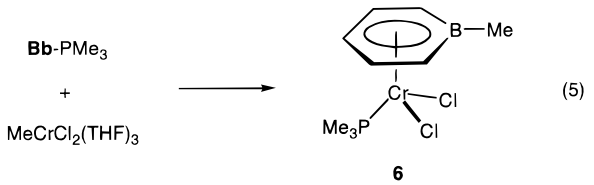

low (16%). No reaction is observed with **Bb**−PMe_3 when $MeCrCl_2(THF)_3$ is pretreated with excess PMe_3 or pyridine (Py). This inability to react in the presence of additional base is consistent with the intramolecular nucleophilic substitution mechanism proposed for the conversion of borabenzene adducts to boratabenzene ligands by transition-metal alkyls.[22]

Treatment of $MeCrCl_2(THF)_3$ with the pyridine adduct of borabenzene, C_5H_5B−NC_5H_5 (**Bb**-Py), under various conditions did not give satisfactory results. Instead, one of the products observed in the reaction is the binuclear dimer [(C_5H_5B−Me)CrClMe]$_2$ (**7** in eq 6),

(20) (a) Ashe, A. J., III; Kampf, J. W.; Müller, C.; Schneider, M. *Organometallics* **1996**, *15*, 387. (b) Ashe, A. J., III; Kampf, J. W.; Wass, J. R. *Organometallics* **1997**, *16*, 163. (c) See also ref 12.

(21) Nishimura, K.; Kuribayashi, H.; Yamamoto, A.; Ikeda, S. *J. Organomet. Chem.* **1972**, *37*, 317.

(22) Putzer, M. A.; Rogers, J. S.; Bazan, G. C. *J. Am. Chem. Soc.* **1999**, *121*, 8112.

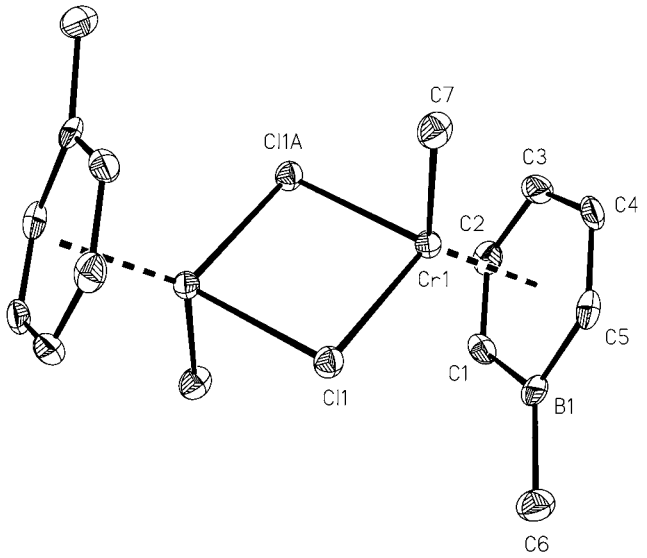

Figure 4. ORTEP view of **7**. Thermal ellipsoids are shown at the 30% probability level; hydrogen atoms were omitted for clarity. Select bond distances (Å): Cr(1)−B(1), 2.524(4); Cr(1)−C(1), 2.445(4); Cr(1)−C(2), 2.354(4); Cr(1)−C(3), 2.230(4); Cr(1)−C(4), 2.255(4); Cr(1)−C(5), 2.297(4); Cr(1)−C(7), 2.065(4); Cr(1)−Cl(1), 2.3542(10); B(1)−C(6), 1.574(6).

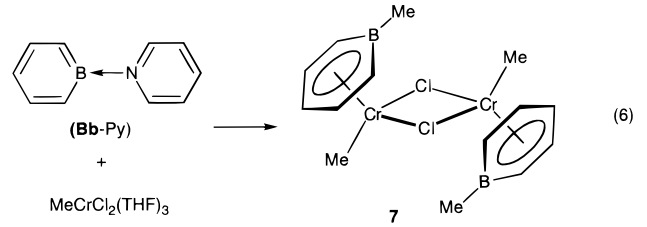

as determined by X-ray diffraction (Figure 4). The molecular structure of **7** contains a crystallographically imposed C_2 axis and is similar in geometry to its Cp analogue.[23] It should be noted that the yield of **7** is low (∼5%) and that the reaction produces multiple products, based on the different colored fractions obtained by extraction with solvents of varying polarity. Efforts to improve the yield of **7** by increasing the scale of the reaction or by using 2 equiv of $MeCrCl_2(THF)_3$ and **Bb**−Py or **Bb**−PMe_3 failed. The presence of two methyl fragments in **7** suggests redistribution reactions among chloride and methyl ligands. These processes may account for the fact that the target product, namely $(C_5H_5B-Me)CrCl_2(Py)$, is not obtained and argue in favor of using homoleptic complexes to maximize reaction yields.

Pyridine Adducts. Treatment of $CrCl_3(THF)_3$ with 3 equiv of MeMgBr in THF followed by addition of **Bb**−Py gives $(C_5H_5B-Me)CrMe_2(Py)$ (**8** in eq 7) as long purple needlelike crystals from pentane. Yields of **8** improve from 30% to 54% when additional pyridine (∼20 equiv) is added to the reaction mixture after the addition of **Bb**−Py. Figure 5 shows the molecular structure of **8** and confirms the close structural relationship to **2**. The ^{11}B NMR spectrum of **8** displays a broad resonance centered at δ 231 ppm.

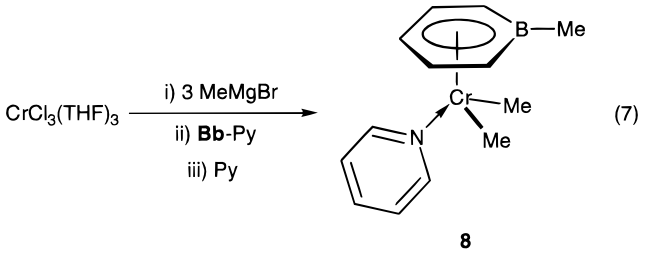

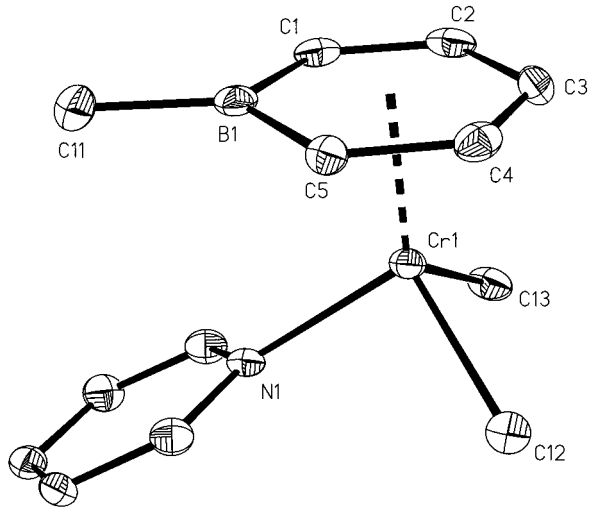

Figure 5. ORTEP view of **8**. Thermal ellipsoids are shown at the 30% probability level; hydrogen atoms were omitted for clarity. Select bond distances (Å): Cr(1)−B(1), 2.531-(3); Cr(1)−C(1), 2.397(3); Cr(1)−C(2), 2.337(2); Cr(1)−C(3), 2.297(3); Cr(1)−C(4), 2.330(3); Cr(1)−C(5), 2.401(3); Cr(1)−C(12), 2.067(3); Cr(1)−C(13), 2.066(3); Cr(1)−N(1), 2.078(3).

Slow addition of 3 equiv of PhMgBr to a slurry of $CrCl_3(THF)_3$ in THF at −45 °C gives rise to a red solution of $Ph_3Cr(THF)_3$.[9] Subsequent addition of **Bb**−Py produces a slow darkening of the solution to a dark brown color. Workup of the reaction by removal of the THF and extraction with toluene give a brown solid. Recrystallization by slow cooling of a pentane/Et_2O solution gives red-brown crystals in 38% yield which are analyzed correctly for $C_{28}H_{25}BCrN$. We propose that the product of the reaction is $(C_5H_5B-Ph)CrPh_2(Py)$ (**9**), as shown in eq 8. The ^{11}B NMR spectrum of **9** displays a resonance centered at δ 316 ppm.

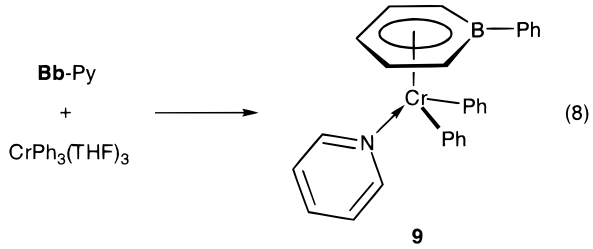

Activation and Reactivity with Ethylene. We previously reported that **1** and **2** in combination with the activators methylaluminoxane (MAO), $B(C_6F_5)_3$, and $[Ph_3C][B(C_6F_5)_4]$[24] polymerize ethylene with catalytic activities competitive with those of group 4 metallocene initiators (eq 9).[6] In this section we provide a more complete account on how different ligand combinations influence the reactivity at chromium. In addition to the

(23) Richeson, D. S.; Hsu, S.; Fredd, N. H.; Van Duyne, G.; Theopold, K. H. *J. Am. Chem. Soc.* **1986**, *108*, 8273.
(24) Chien, J. C.; Tsai, W.; Rausch, M. D. *J. Am. Chem. Soc.* **1991**, *113*, 8570.

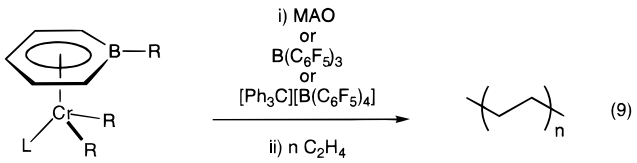

(9)

study of **1**, **2**, **6**, and **8**, we include the compounds $Cp^*CrMe_2(PMe_3)$ and Cp_2ZrCl_2 for reference. The reactivity observed using well-defined activators is presented first, followed by the polymerization reactivity observed using MAO.

Table 1 shows the results from a series of polymerization experiments using $B(C_6F_5)_3$ and $[Ph_3C][B(C_6F_5)_4]$ ($[Cr] = 1 \times 10^{-3}$ M, 30 min reaction time, 23 °C, 1 atm of C_2H_4). Compound **2** reacts with $B(C_6F_5)_3$ in toluene, and an immediate color change from purple to dark green is observed. Stirring solutions of **2** and $B(C_6F_5)_3$ under ethylene results in the immediate precipitation of polyethylene. Better results are observed with a $B(C_6F_5)_3$ to **2** ratio of 2 (entries 2−4). Excellent activity is also observed with **2**/$[Ph_3C][B(C_6F_5)_4]$ (entry 5). Compound **1** and $B(C_6F_5)_3$ fail to give an active catalyst (entry 1).

The reaction of **8** with $B(C_6F_5)_3$ or $[Ph_3C][B(C_6F_5)_4]$ in toluene also results in a green solution. The **8**/$B(C_6F_5)_3$ combination gives activities comparable with that of **2**/$B(C_6F_5)_3$ (entries 2, 3, 6, and 7 in Table 1). In contrast to **2**, the use of *n* $B(C_6F_5)_3$ ($n = 1, 2$) with **8** leads to polymers with a broad molecular weight distribution. Figure 6 shows the gel permeation chromatography (GPC) trace of the polymer corresponding to entry 6 in Table 1. The combination **8**/$[Ph_3C][B(C_6F_5)_4]$ leads to a catalyst with lower overall activity (entry 8); however, the resulting polymer exhibits a monomodal distribution (Figure 7). Note that the molecular weight of this polyethylene is approximately twice that of the polymer obtained using **2**/$[Ph_3C][B(C_6F_5)_4]$ (entry 5). Finally, the activity obtained using $Cp^*CrMe_2(PMe_3)/B(C_6F_5)_3$ (entry 9) is within the same order of magnitude as those obtained with the boratabenzene counterparts. In all cases, melting points typical for linear polyethylene were obtained. Compounds **2** and **8** in combination with $B(C_6F_5)_3$ or $[Ph_3C][B(C_6F_5)_4]$ at lower concentrations ($[Cr] = 10^{-4}$ or 10^{-5} M) failed to give active catalysts under our experimental conditions.

Table 2 summarizes the ethylene polymerization experiments conducted in the presence of MAO under various concentrations (Al/M = 1000; M = Cr, Zr; 30 min reaction time; 1 atm of C_2H_4). It should be noted that the Py adducts, i.e., **8**/MAO and **9**/MAO, do not provide polymerization catalysts. As shown by entries 1 and 2, for the case of **1**/MAO, reducing the concentration of Cr results in a greater activity per metal site. This trend is also apparent when using **2** (entries 3, 5, and 6). Catalysts derived from **6**/MAO and **2**/MAO give comparable activities and polymers with similar properties (entries 3 and 4). Using **1**/MAO, one obtains a polymer with a molecular weight about twice that obtained with **2**/MAO (entries 2 and 6). The GPC traces for the polymers obtained from entries 2 and 6, provided in Figures 8 and 9, respectively, show monomodal molecular weight distributions. Higher molecular weights and activities are observed with Cp_2ZrCl_2/MAO under our experimental conditions. The reactivity of $Cp^*CrMe_2(PMe_3)$/MAO with ethylene under conditions similar to that of the boratabenzene complexes is noteworthy. At high concentrations, rapid monomer consumption is observed, but only soluble products are obtained (entry 7).[25] Under dilute conditions, the activity of $Cp^*CrMe_2(PMe_3)$/MAO is high and polyethylene is formed. However, the molecular weight of the polymer produced remains low relative to the polymer obtained using the boratabenzene complexes (entry 8).

Catalyst Lifetime. A catalyst's ability to consume monomer over time is an important parameter to evaluate its potential. The activities reported in Tables 1 and 2 are averaged over a 30 min period. To monitor the relative rate of ethylene consumption as a function of time, the time required for a given catalyst solution to consume 1.0 mL of ethylene was measured at different intervals. A shift to longer consumption times reflects catalyst degradation.

Figure 10 shows the activity versus time relation for **2**/$B(C_6F_5)_3$, **2**/2 $B(C_6F_5)_3$, **2**/$[Ph_3C][B(C_6F_5)_4]$, and **2**/MAO under similar reaction conditions ($[Cr] = 1 \times 10^{-3}$ M, 1 atm of C_2H_4). The best stability is found using **2**/MAO, which maintains ~35% of its initial activity after 2 h. Activation with 2 equiv of $B(C_6F_5)_3$ also gives a robust system. Figure 11 illustrates the same experiments using **8** and various cocatalysts. Since the **8**/MAO combination does not result in a catalyst, it was omitted from this study. Similar to the reactions with **2**, the better uptake is found with **8**/2 $B(C_6F_5)_3$. Unlike the stability of **2**/$[Ph_3C][B(C_6F_5)_4]$, a rapid decrease in ethylene consumption is observed using **8**/$[Ph_3C][B(C_6F_5)_4]$.

Conclusion

Efforts to synthesize Cr(III) complexes by using boratabenzene salts invariably led to metal reduction. To date, the borabenzene−adduct route remains the only viable method for their synthesis. Unfortunately, this method does not enable the preparation of complexes supported by boratabenzene ligands with boron substituents that can participate in π-bonding. The range of reactivities observed with different bis(boratabenzene)zirconium dichloride precursors has, therefore, not been attained with boratabenzene−chromium catalysts.

As shown by the phosphine complex **2** and the pyridine-containing analogue **8**, there is some structural flexibility. Our observations indicate that the phosphine ligand coordinates more tightly to chromium, giving higher synthetic yields and more robust catalysts. The catalysts containing a phosphine ligand also yield polymers with narrower molecular weight distributions. That **8**/MAO fails to polymerize ethylene suggests that the pyridine is removed by the aluminum species in MAO, rendering chromium inactive. Pyridine abstraction seems likely in light of Theopold's use of trimethylaluminum to prepare $[Cp^*CrMe_2]_2$ from $Cp^*CrMe_2(Py)$.[26] For those combinations that provide polymerization catalysts, their performance is competitive with those observed with Cp_2ZrCl_2 and $Cp^*CrMe_2(PMe_3)$.

In comparison to $Cp^*CrMe_2(PMe_3)$/MAO, the combinations with boratabenzene complexes lead to higher

(25) Rogers, J. S.; Bazan, G. C. *Chem. Commun.* **2000**, 1209.
(26) Noh, S. K.; Sendlinger, S. C.; Janiak, C.; Theopold, K. H. *J. Am. Chem. Soc.* **1989**, *111*, 9127.

Table 1. Ethylene Polymerization Results with Well-Defined Boron Activators

entry	precatalyst	activator	activity[a]	$10^{-3}M_n$	$10^{-3}M_w$	PDI[b]	T_m
1	**1**	$B(C_6F_5)_3$	0				
2	**2**	$B(C_6F_5)_3$	28	10.6	45.5	4.29	127.4
3	**2**	2 $B(C_6F_5)_3$	72	16.6	53.9	3.25	128.7
4	**2**	3 $B(C_6F_5)_3$	65.9	13.8	59.8	4.33	129.7
5	**2**	$[Ph_3C][B(C_6F_5)_4]$	51	39.5	114	2.89	130.0
6	**8**	$B(C_6F_5)_3$	26	9.0	322	35.9	129.7
7	**8**	2 $B(C_6F_5)_3$	65	10.0	217	21.7	129.2
8	**8**	$[Ph_3C][B(C_6F_5)_4]$	23	85.4	229	2.68	129.9
9	$Cp^*CrMe_2(PMe_3)$	$B(C_6F_5)_3$	44	14.7	56.7	3.87	129.5

[a] Activity measured in kg of product/((mol of Cr) h). [b] PDI = M_w/M_n.

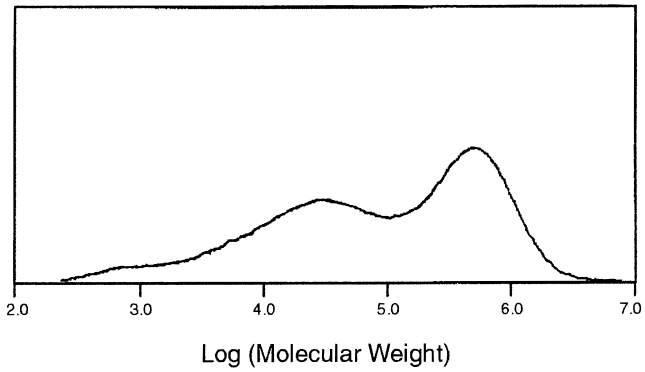

Figure 6. Gel permeation chromatography (GPC) trace of the polymer obtained using **8**/$B(C_6F_5)_3$.

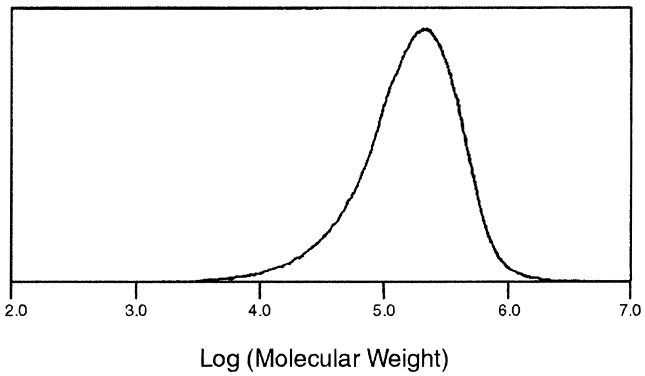

Figure 7. GPC trace of the polymer obtained using **8**/$[Ph_3C][B(C_6F_5)_4]$.

molecular weight polymers. With the zirconium catalysts $Cp^*_2ZrCl_2$/MAO and $(C_5H_5B{-}OEt)_2ZrCl_2$/MAO, one observes the opposite trend, with the boratabenzene catalyst producing lower molecular weight product as a result of increased rates of β-H elimination.[7] The presence of odd-carbon products[25] in the reactions of $Cp^*CrMe_2(PMe_3)$/MAO suggests that polymer growth is restricted by transmetalation reactions between chromium and Al−Me functionalities in MAO.[27] It is not clear at this stage why chain transfer to aluminum is slower for the boratabenzene counterparts.

Experimental Section

General Remarks. All manipulations were performed under an inert atmosphere using standard glovebox and vacuum-line techniques.[28] $CrCl_3(THF)_3$,[29] $MeCrCl_2(THF)_3$,[21] Li($C_5H_5B{-}NMe_2$),[30] **Bb**−PMe_3,[8b] **Bb**−Py,[8b] **1**,[6] **2**,[6] $B(C_6F_5)_3$,[31] and $[Ph_3C][B(C_6F_5)_4]$[24] were prepared according to literature methods. MeMgBr (3.0 M in Et_2O) and PhMgBr (1.0 M in Et_2O) were purchased from Aldrich and used as received. Toluene, benzene, THF, pentane, and Et_2O were distilled from sodium benzophenone ketyl. Pyridine was dried over 3 Å molecular sieves and distilled under vacuum. MAO, 10.3 wt % Al in toluene, was purchased from Akzo Nobel Chemicals, Inc., and used as received. NMR spectra were obtained using a Varian Unity 400 or 500 spectrometer. ^{1}H NMR spectra were calibrated using signals from the solvent and are reported downfield from $SiMe_4$. ^{11}B NMR spectra were calibrated and reported downfield from external $BF_3{\cdot}OEt_2$. Elemental analyses were performed by Desert Analytics, Inc., Tucson, AZ. DSC measurements were recorded using a Perkin-Elmer DSC Pyris 1. GPC experiments were performed with a Waters 150C GPC instrument at 140 °C using 1,2,4-trichlorobenzene as the solvent.

($C_5H_5B{-}NMe_2)_2Cr$ (4). $CrCl_3(THF)_3$ (334 mg, 0.891 mmol) was suspended in 2 mL of THF at room temperature. A solution of Li($C_5H_5B{-}Me$) (113 mg, 0.890 mmol) in 4 mL of THF was slowly added, resulting in a red solution. The volatiles were removed in vacuo, and the resulting solid was extracted with pentane and filtered through Celite. Removal of pentane in vacuo resulted in bright red crystals of **4**. This solid was recrystallized from pentane (79 mg, 0.27 mmol, 60%). ^{1}H NMR (C_6D_6, 400 MHz): δ 58.0 (br, 12H, $N(CH_3)_2$). HRMS-EI: calcd ($C_{14}H_{22}B_2CrN_2$), 292.1374; found, 292.1397.

($C_5H_5B{-}Me)CrCl_2(PMe_3)$ (6). Bb−PMe_3 (173 mg, 1.14 mmol) was placed in a 100 mL round-bottom flask with 5 mL of benzene and a magnetic stir bar. This mixture was stirred until dissolved. $MeCrCl_2(THF)_3$ (393 mg, 1.11 mmol) was then added as a solid all at once, and the solution became dark blue-green immediately. The mixture was stirred for 5 min, and the volatiles were removed in vacuo. The resulting solid was washed with pentane (4 × 15 mL) and then extracted with 6 mL of toluene. Filtration and evaporation of toluene gave 170 mg of a blue-black solid. The product was crystallized from 3 mL of toluene to give dark blue crystals of **6** in low yield (51 mg, 0.18 mmol, 16%). ^{1}H NMR (C_6D_6, 400 MHz): δ −52.4 (br, 9H, $P(CH_3)_3$), −28.8 (br, 3H, BCH_3). IR (KBr plates, C_6H_6, cm^{-1}): 609, 689, 747, 867, 955, 1108, 1285, 1414, 1478, 1513, 2985, 3064. Anal. Calcd for $C_9H_{17}BCl_2CrP$: C, 37.29; H, 5.91; Cl, 24.46. Found: C, 37.20; H, 5.87; Cl, 24.22.

Observation of $[(C_5H_5B\text{-}Me)CrMe(\mu\text{-}Cl)]_2$ (7). A solution of **Bb**−Py (118 mg, 0.759 mmol) in 4 mL of toluene was added dropwise to a slurry of $MeCrCl_2(THF)_3$ (268 mg, 0.756 mmol) in 2 mL of toluene. The solution remained dark green. After the mixture was stirred for 10 min, the volatiles were removed in vacuo. The residue was extracted with pentane, filtered, and cooled to −35 °C. Dark green crystals formed overnight. ^{1}H NMR (C_6D_6, 400 MHz): δ −7.6 (br, 3H, BCH_3).

(27) Chain transfer to aluminum also occurs with iron-based catalysts; see: Britovsek, G. J. P.; Bruce, M.; Gibson, V. C.; Kimberley, B. S.; Maddox, P. J.; Mastroianni, S.; McTavish, S. J.; Redshaw, C.; Solan, G. A.; Strömberg, S.; White, A. J. P.; Williams, D. J. *J. Am. Chem. Soc.* **1999**, *121*, 8728.

(28) Burger, B. J.; Bercaw, J. E. In *Experimental Organometallic Chemistry*; Wayda, A. L., Darensbourg, M. Y., Eds.; ACS Symposium Series 357; American Chemical Society: Washington, DC, 1987.

(29) Herwig, W.; Zeiss, H. H. *J. Org. Chem.* **1958**, *23*, 1404.

(30) Qiao, S.; Hoic, D. A.; Fu, G. C. *J. Am. Chem. Soc.* **1996**, *118*, 2291.

(31) Massey, A. G.; Park, A. J. *J. Organomet. Chem.* **1964**, *2*, 245.

Table 2. Polymerization Results Using MAO Cocatalyst

entry	precatalyst	[M] (M)	activity[a]	$10^{-3}M_n$	$10^{-3}M_w$	PDI[b]	T_m (°C)
1	**1**	10^{-3}	72	6.46	28.7	4.43	130.2
2	**1**	10^{-5}	3640	53.1	123	2.32	133.7
3	**2**	10^{-3}	86	3.13	11.6	3.71	128.0
4	**6**	10^{-3}	83	2.97	12.1	4.07	130.5
5	**2**	10^{-4}	1020	15.8	41.7	2.64	131.7
6	**2**	10^{-5}	4040	27.6	61.8	2.24	132.7
7	$Cp^*CrMe_2(PMe_3)$[c]	10^{-3}	74				
8	$Cp^*CrMe_2(PMe_3)$	10^{-5}	5310	3.91	19.0	4.87	130.3
9	Cp_2ZrCl_2	10^{-3}	85	9.87	22.3	2.55	132.5
10	Cp_2ZrCl_2	10^{-5}	5210	255	809	3.17	135.0

[a] Activity measured in kg of product/((mol of M) h). [b] M_w/M_n. [c] Only soluble *n*-alkanes were obtained from this reaction.

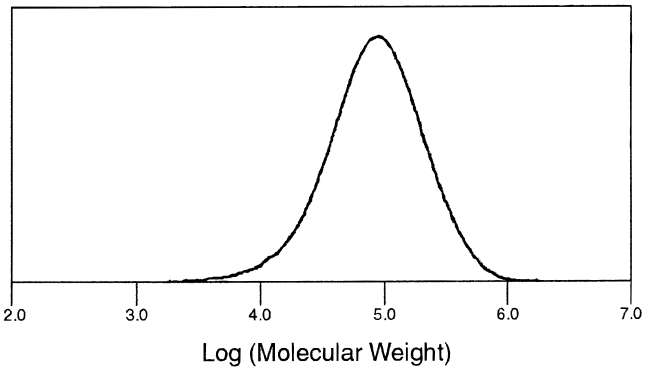

Figure 8. GPC trace of the polymer obtained using **1**/MAO.

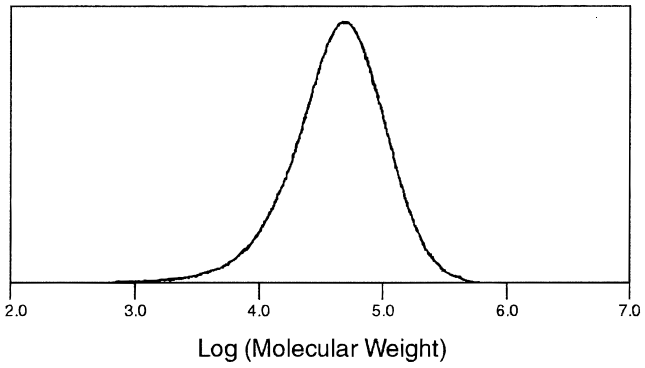

Figure 9. GPC trace of the polymer obtained using **2**/MAO.

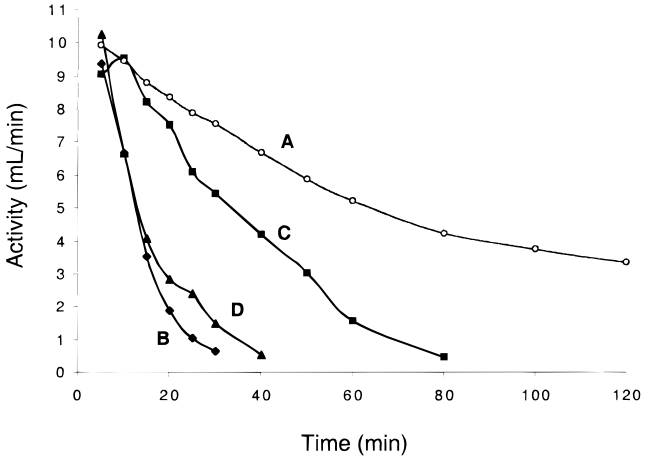

Figure 10. Relative activity versus time using **2** and (A) MAO, (B) $B(C_6F_5)_3$, (C) $2B(C_6F_5)_3$, and (D) $[Ph_3C][B(C_6F_5)_4]$.

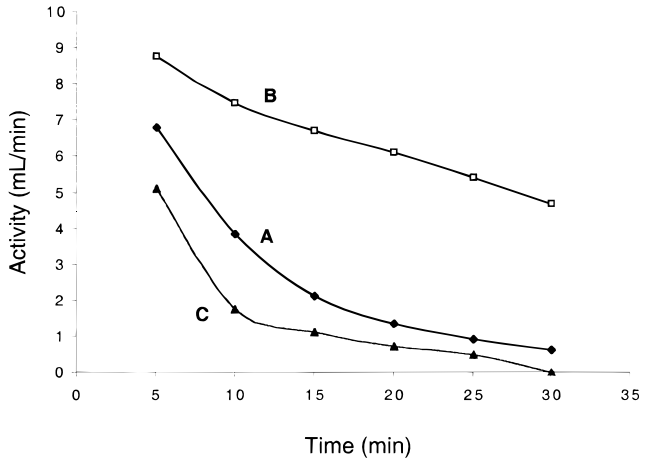

Figure 11. Relative activity versus time using **8** and (A) $B(C_6F_5)_3$, (B) $2B(C_6F_5)_3$, and (C) $[Ph_3C][B(C_6F_5)_4]$.

(C_5H_5B−Ph)$CrPh_2$(Py) (9). $CrCl_3(THF)_3$ (373 mg, 0.996 mmol) was placed in a 250 mL sidearm flask with 15 mL of THF and a stir bar. The flask was fitted with an addition funnel containing 10 mL of THF and PhMgBr (2.99 mL, 2.99 mmol) and was cooled to −45 °C (dry ice/acetonitrile) under argon. The addition was performed over a 30 min period and the solution changed from purple to brown, then green, and finally bright red. The mixture was then stirred at −45 °C for an additional 3 h. A solution of **Bb**−Py (155 mg, 0.997 mmol) in 10 mL of THF was added dropwise via syringe. The solution became brown within minutes and was held at −45 °C for 30 min. The mixture was warmed to room temperature for an additional 30 min, and the volatiles were removed in vacuo. The product was extracted with toluene, filtered, and evaporated to dryness. The residue was extracted with Et_2O, filtered, and cooled to −35 °C, giving red-brown crystals of **9** (167 mg, 0.382 mmol, 38%). ^1H NMR (C_6D_6, 400 MHz): δ 1.4 (br), 3.6 (br), 6.5 (br), 10.6 (br), 14.7 (br), 16.3 (br). ^{11}B NMR (C_6D_6, 128 MHz): δ 316. Anal. Calcd for $C_{28}H_{25}BCrN$: C, 76.73; H, 5.75; N, 3.20. Found: C, 73.46; H, 5.38; N, 3.45.

(C_5H_5B−Me)$CrMe_2$(Py) (8). Method A. $CrCl_3(THF)_3$ (371 mg, 0.990 mmol) was placed in a 250 mL sidearm flask with 20 mL of THF and a stir bar. The flask was fitted with an addition funnel containing 10 mL of THF and MeMgBr (0.99 mL, 2.97 mmol). The flask was cooled to −45 °C (dry ice/acetonitrile) under argon. The addition was performed over a 30 min period, and the mixture was stirred at −45 °C for an additional 3 h. A solution of **Bb**−Py (154 mg, 0.994 mmol) in 15 mL of THF was added dropwise via syringe. The solution became dark green within minutes and was held at −45 °C for 30 min. The mixture was warmed to room temperature for an additional 30 min, becoming purple-black. Volatiles were removed in vacuo, and the product was extracted with 50 mL of pentane. The solution was filtered through Celite and washed twice with pentane. The pentane was evaporated to dryness, and the purple-black crystals were recrystallized from 7 mL of pentane, giving fine, purple-black needles (75 mg, 0.298 mmol, 30%). ^1H NMR (C_6D_6, 400 MHz): δ −9.0 (br), 17.7 (br). ^{11}B NMR (C_6D_6, 128 MHz): δ 231 (s, br). IR (KBr plates,

Table 3. Summary of Crystallographic Data for 3−5

	3	4	5
empirical formula	$C_{12}H_{16}B_2Cr$	$C_{14}H_{22}B_2CrN_2$	$C_{22}H_{20}B_2Cr$
fw	233.87	291.96	358.00
temp (K)	150	150	193(2)
wavelength (Å)	0.710 73	0.710 73	0.710 73
cryst syst	monoclinic	monoclinic	monoclinic
space group	$P2_1/c$	$C2/c$	$P2_1/n$
unit cell dimens			
a (Å)	6.761(2)	32.785(6)	13.1282(6)
b (Å)	8.039(2)	10.569(2)	26.6304(12)
c (Å)	11.086(3)	8.317(2)	13.3940(6)
β (deg)	104.315(3)	94.920(3)	104.6450(10)
V (Å^3), Z	583.9(2), 2	2871.3(10), 8	4530.5(4), 10
calcd density (Mg/m^3)	1.330	1.351	1.312
abs coeff (mm^{-1})	0.939	0.782	0.631
F(000)	244	1232	1860
cryst size (mm)	0.33 × 0.27 × 0.13	0.40 × 0.40 × 0.067	
θ range for data collection (deg)	3.11−25.00	1.25−25.00	1.53−23.28
limiting indices	$-8 \le h \le 8$, $-10 \le k \le 10$, $-14 \le l \le 14$	$-43 \le h \le 43$, $-13 \le k \le 14$, $-10 \le l \le 11$	$-14 \le h \le 14$, $-27 \le k \le 29$, $-14 \le l \le 11$
no. of rflns collected	4906	12 276	17 676
no. of indep rflns	1028 (R(int) = 0.0277)	2525 (R(int) = 0.0338)	6273 (R(int) = 0.0543)
refinement method		full-matrix least-squares on F^2	
no. of data/restraints/params	1027/0/71	2523/0/176	6273/0/565
goodness of fit on F^2	1.080	0.962	1.143
final R indices ($I > 2\sigma(I)$)	R1 = 0.0266, wR2 = 0.0759	R1 = 0.0283, wR2 = 0.0846	R1 = 0.0748, wR2 = 0.1312
R indices (all data)	R1 = 0.0287, wR2 = 0.0776	R1 = 0.0414, wR2 = 0.1010	R1 = 0.1131, wR2 = 0.1452
largest diff peak and hole (e Å^{-3})	0.280 and −0.314	0.266 and −0.285	0.245 and −0.362

Table 4. Summary of Crystallographic Data for 6−8

	6	7	8
empirical formula	$C_{12}H_{20}BCl_2CrP$	$C_{14}H_{22}B_2Cl_2Cr_2$	$C_{13}H_{19}BCrN$
fw	289.92	386.84	252.10
temp (K)	150	293(2)	150
wavelength (Å)	0.710 73	0.710 73	0.710 73
cryst syst	monoclinic	monoclinic	orthorhombic
space group	$P2_1/n$	$P2_1/n$	$Pca2_1$
unit cell dimens			
a (Å)	10.107(2)	7.2105(10)	7.8760(8)
b (Å)	6.5117(14)	6.9126(9)	10.9795(11)
c (Å)	24.653(5)	17.357(2)	15.303(2)
β (deg)	94.761(4)	90.077(2)	90
V (Å^3), Z	1616.9(6), 4	865.1(2), 2	1323.3(2), 4
calcd density (Mg/m^3)	1.351	1.485	1.265
abs coeff (mm^{-1})	1.114	1.550	0.837
F(000)	680	396	532
cryst size (mm)	0.33 × 0.11 × 0.040	0.29 × 0.11 × 0.013	0.39 × 0.07 × 0.53
θ range for data collection (deg)	1.66−25.00	2.35−23.29	1.85−25.00
limiting indices	$-13 \le h \le 13$, $-8 \le k \le 8$, $-31 \le l \le 32$	$-8 \le h \le 7$, $-7 \le k \le 4$, $-19 \le l \le 18$	$-10 \le h \le 10$, $-14 \le k \le 14$, $-20 \le l \le 19$
no. of rflns collected	13 812	3693	11 072
no. of indep rflns	2853 (R(int) = 0.0850)	1240 (R(int) = 0.0541)	2308 (R(int) = 0.0619)
refinement method		full-matrix least-squares on F^2	
no. of data/restraints/params	2847/0/190	1240/0/135	2307/1/149
goodness of fit on F^2	1.023	0.857	0.958
final R indices ($I > 2\sigma(I)$)	R1 = 0.0536, wR2 = 0.1295	R1 = 0.0316, wR2 = 0.0615	R1 = 0.0327, wR2 = 0.0633
R indices (all data)	R1 = 0.0755, wR2 = 0.1390	R1 = 0.0435, wR2 = 0.0637	R1 = 0.0456, wR2 = 0.0671
largest diff peak and hole (e Å^{-3})	0.812 and −0.812	0.350 and −0.390	0.410 and −0.183

C_6H_6, cm^{-1}): 697, 760, 1059, 1102, 1298, 1415, 1442, 1515, 1599, 2868, 2918. Anal. Calcd for $C_{13}H_{19}BCrN$: C, 61.93; H, 7.60; N, 5.56. Found: C, 62.14; H, 7.39; N, 5.58.

Method B. The above experiment was repeated using $CrCl_3(THF)_3$ (594 mg, 1.59 mmol), MeMgBr (1.59 mL, 4.77 mmol), and **Bb**−Py (246 mg, 1.59 mmol). After the mixture was stirred for an additional 30 min at −45 °C, pyridine (3 mL, 2.9 g, 37 mmol) in 3 mL of THF was added dropwise. This solution was stirred for 30 min at −45 °C and slowly warmed to room temperature. Workup in the same manner as above gave crystalline **8** (216 mg, 0.858 mmol, 54%).

Structure Determinations. Crystal data are summarized in the following appendices. Crystals were mounted under Paratone-8277 onto a glass fiber or cactus needle and immediately placed in a cold nitrogen stream at −80 or −120 °C on the X-ray diffractometer. The X-ray intensity data were collected on a standard Siemens SMART CCD area setector system equipped with a normal-focus molybdenum-target X-ray tube operated at 2.0 kW (50 kV, 40 mA). Laue symmetry was used to reveal the crystal system, and the final unit cell parameters (at −80 °C) were determined from the least-squares refinement of three-dimensional centroids.[32] Data were corrected for absorption with the SADABS[33] program.

The space group was assigned, and the structure was solved by using direct methods and refined employing full-matrix least-squares on F^2 (Siemens, SHELXTL,[34] version 5.04). All of the non-H atoms were refined with anisotropic thermal parameters, unless otherwise noted. Hydrogen atoms were

included in idealized positions, giving a data to parameter ratio of greater than 10:1. The structures were refined to goodness of fit (GOF)[35] and final residuals.[36] The crystal data and refinement results for **3**−**5** are summarized in Table 3, and data for **6**−**8** are provided in Table 4. Positional coordinates, selected bond distances and angles, anisotropic displacement parameters, and hydrogen atom positions are tabulated in the Supporting Information.

General Polymerization Procedure. In the glovebox, 50 μmol of the precatalyst was weighed to the nearest 0.1 mg and dissolved in toluene. Stock solutions of the precatalysts (5.00 μmol/g) were used for more dilute polymerizations ([M] = 10^{-4} and 10^{-5} M). The complexes were combined with the appropriate amount of MAO (1000 Al/M), $B(C_6F_5)_3$ (1 or 2 equiv), or $[Ph_3C][B(C_6F_5)_4]$ (1.0 equiv) and placed in a 100 mL round-bottom flask with a stir bar. Enough toluene was added to bring the total volume to 50 mL. The flask was fitted with a needle valve assembly and removed from the glovebox. The mass of the apparatus was recorded to the nearest 0.001 g and placed on a Schlenk line equipped with an ethylene manifold. Vacuum was applied for 5 s, and the flask was placed in a room-temperature water bath. The flask was opened to the ethylene source vented to a mercury bubbler. After 30 min of reaction, the flask was cleaned and weighed again to the nearest 0.001 g for activity measurements. The reaction was quenched using 3 mL of water, and alumina salts were dissolved in aqueous base for the reaction using MAO activator. Reactions using borane or borate activators were quenched with 5 mL of acetone, and these mixtures were stirred for 30 min. The toluene layer was extracted, filtered, and placed under vacuum overnight to give the product.

Acknowledgment. We are grateful to the Department of Energy, the Petroleum Research Fund, administered by the American Chemical Society, and Equistar Chemicals LP for financial assistance.

Supporting Information Available: Complete details for the crystallographic studies of **3**−**8**. This material is available free of charge via the Internet at http://pubs.acs.org.

OM0003685

(32) It has been noted that the integration program SAINT produces cell constant errors that are unreasonably small, since systematic error is not included. More reasonable errors might be estimated at 10× the listed value.

(33) The SADABS program is based on the method of Blessing; see: Blessing, R. H. *Acta Crystallogr., Sect A* **1995**, *51*, 33.

(34) SHELXTL: Structure Analysis Program, version 5.04; Siemens Industrial Automation Inc., Madison, WI, 1995.

(35) GOF = $[\sum[w(F_o^2 - F_c^2)^2]/(n - p)]^{1/2}$, where n and p denote the number of data and parameters, respectively.

(36) R1 = $\sum(||F_o| - |F_c||)/\sum|F_o|$; wR2 = $[\sum w(F_o^2 - F_c^2)^2]/[\sum w(F_o^2)^2]]^{1/2}$, where $w = 1/[\sigma^2(F_o^2) + (aP)^2 + bP]$ and $P = [(\text{Max}; 0, F_o^2) + 2F_c^2]/3$.